



DIAMOND TOOL WEAR ANALYSIS DURING MACHINING OF MICROSTRUCTURE SURFACE FOR MICROINJECTION MOLDING

Renato Goulart Jasinevicius

Laboratório de Engenharia de Precisão, Departamento de Engenharia Mecânica, Escola de Engenharia de São Carlos, Universidade de São Paulo, C.P. 359, CEP 13566-590, São Carlos, São Paulo, Brazil. † Corresponding author: renatogj@sc.usp.br

Renaê Mendes Granado

Instituto de Matemática e Estatística-CTC-UERJ, CEP 20550-013, Rio de Janeiro, Brasil. rmgra@ig.com.br

Giuseppe Antonio Cirino

Centro de Ciências Exatas e de Tecnologia – CCET, Universidade Federal de São Carlos, CEP 13560-905 São Carlos, São Paulo, Brazil

Abstract. Tool wear is one of the main issues concerning the economics of a machining process. The purpose of this paper is to discuss the wear mechanism of a monocrystalline diamond tool with a special geometry used to machine a commercially pure copper insert and the wear effect on the machined surface. The cutting tests were performed on a two-axis ultraprecision turning machining. The cutting tool wear pattern was investigated based upon the observation of the worn region using scanning electron microscopy. The examination of the tool wear showed that the wear was present after a short cutting distance (2.5 km). The zero degree rake angle single point diamond tool presented a small notch on the flank face. No wear was detected on the rake face of the diamond tool. The possible wear mechanisms that affected the tool performance and surface generation were discussed. The machined surface presented a microhardness alteration. It is believed that oxidation and work hardening induced by machining are responsible for the uneven wear along the cutting edge.

Keywords: Ultraprecision, wavefront sensor, mold insert, microstructure, diamond tool wear

1. INTRODUCTION

The application of single point diamond turning for the fabrication of non-ferrous metals' inserts for micro injection moulding has been established as an important technology for the replication of small optical components such as diffraction optical elements (DOE) (Davies et al, 2003; Yoshikawa et al, 2009; Falldorf et al, 2008; Tofteberg et al 2008; and Sahli et al 2009). Examples of diffraction optical elements are Fresnel lenses, blaze gratings, phase gratings etc (Leung et al, 2009; Rakuff and Beaudet, 2008). The manufacturing of micro-lens inserts with an aspherical profile is one of the major fields demanding this machining technology according to Yoshikawa et al (2009).

The geometry of the cutting tools used to manufacture DOE differs from those used for conventional ultraprecision contour machining because in that the point radius is generally very small. All those unconventional tool point are manufactured in order to attend the demand for fabrication of special micro features onto surfaces such as a Fresnel lens. According to Qin et al (2010) special tool shapes used to fabricate microstructures are chevron nosed, "half radius" nosed, facet point tool, etc. Special tool point geometries are required in order to achieve small and intricate features on the surface. Sharpening of these tools is very difficult which implies high costs. The accuracy and the smoothness of the cutting edge are extremely important for a successful machining operation. The sharpness of these cutting tools is extremely fine and their edge radii are in the range of 40 nm or smaller. Consequently, both the chip contact length and the uncut chip thickness are very small intensifying the specific cutting energy.

Although diamond turning is a well established technique for the machining of DOE, some problems may arise in the microcutting process when premature wear takes place in the cutting edge. Furthermore, only few works have reported on the effect of microcutting process upon tool wear in the diamond turning of microstructure (Zhou et al, 2003; Yin et al., 2009; Zhang and Zhou, 2010). According to Zhang and Zhou (2010) in the cutting of microstructured surfaces, diamond tools with small round nose radius are used to avoid cutting interference. The depth of cut changes cyclically along the profile of the cut surfaces. Tool wear patterns may be quite different from conventional diamond turning because of the the special tool geometry and cutting process (idem). A large number of works have addressed diamond tool wear in the machining of non ferrous metals (Bex, 1975; Wong, 1981; Hurt and Decker; 1984, Shimada et al, 2000; and Tanaka et al 2005). High accuracy machining of either large components or a large batch, make low tool wear an essential requirement as discussed by Shimada and collaborators (2000). Papers reporting the wear of diamond tools have mainly focused on the effect of material during machining (Shimada et al 2000) erosion and hertzian test as described by Tanaka et al (2005). Paul and co-workers (1996) have proposed that the relevant factor in chemical wear is the presence of unpaired d-electrons in the sample being turned. Diverse experimental evidence (involving diamond synthesis, coal gasification, and wetting of diamonds by molten metals) supports the conclusion that serves as the basis of a theory of chemical diamond tool wear: unpaired *d* electrons in the workpiece allow carbon-carbon bond breaking in

R.G. Jasinevicius, R.M. Granado and G.A. Cirino
Diamond tool wear analysis

diamond followed by metal-carbon complex formation, leading to chemical wear of diamond tools. Although copper does not present unpaired *d*-electron, metal-carbon-oxygen compounds can form, in the presence of oxygen, which are energetically more stable than metal-carbon compounds. It is known that oxygen is found in commercially pure copper (as an impurity).

In this paper, a very small tool nose radius diamond tool was used to investigate tool wear in the machining of inserts for injection molding of a wavefront sensor (Patent PI0201535 8). The influence of tool wear on the surface roughness within the cutting grooves was also studied.

2. Experimental Details

Single point diamond turning tests were carried out on Aspheric Surface Generator Rank Pneumo ASG 2500. This is a T-base carriage configuration with carriages sliding on hydrostatic bearing, driven by pulse-width-modulated dc servomotors, rotary-to-linear motion through 5 mm pitch ballscrews and position feedback using laser interferometer.

Samples of commercially pure copper were used in the test. The original Vickers microhardness of the three samples were $H_v = 86 \text{ kgf/mm}^2$. In order to study the effect of the work hardening on the machined surface layer, the microhardness of the *as received* sample (polished and etched) and the diamond turned surfaces were measured. Microhardness was measured with a VMHT MET Leica (Leica Mikrosysteme, GmbH; A-1170, Vienna, Austria) micro indentation machine. A diamond Vicker's Hardness indenter was driven into the sample using a cycle time of 15 seconds. Several loads were applied: 5g, 10g, 15g, 25g, 50g, 100g, 200g. Average results of four repeated tests were plotted and compared with the *as received* sample.

The surface roughness of the diamond turned surfaces was examined by a non-contact Wyko NT 1100 (Veeco Metrology Group) surface measurement system, with 50x magnification. The Vertical-shifting interferometry (VSI) mode was chosen in the experiment. The images of the surfaces were then plotted by Vision software from Veeco Instruments, Inc.

Table 1 and Figure 1 describe the cutting conditions and tool geometry used in the tests. Five copper inserts were face cut with constant feedrate of $1 \mu\text{m/rev}$ and depth of cut of $10 \mu\text{m}$. A flat cavity ($100 \mu\text{m}$ deep) was machined before the microfeature (wavefront structure (Patent PI0201535 8) as shown in Figure 2 (a and b); the cutting conditions to provide the microfeatures are the same used for the face cut of the flat cavity. 3D view of the surface topology after machining, and cross-sectional view of the surface roughness profile in the X direction are shown in Figures 2(b) and 2(c). The estimated cutting distance run by the cutting tool was 3 km.

Table 1. Cutting tool and cutting conditions for tool life test

| | |
|--|------------------------------------|
| Cutting tool | |
| Material | Monocrystalline diamond (Sumitomo) |
| Nose radius [mm] | 0.055 |
| Rake | 0° |
| Clearance (primary) | 10° |
| Included Angle | 18° |
| Obs.: Waviness $< 0.25 \mu\text{m}$ over 160° excluding elliptical form | |
| Workpiece | Material Electroless Copper |
| Cutting conditions (wavefront sensor) | |
| Spindle speed [rpm] | 1000 |
| Feed rate [$\mu\text{m}/\text{rev}$] | 1.0 |
| Depth of cut [μm] | 6.4 |

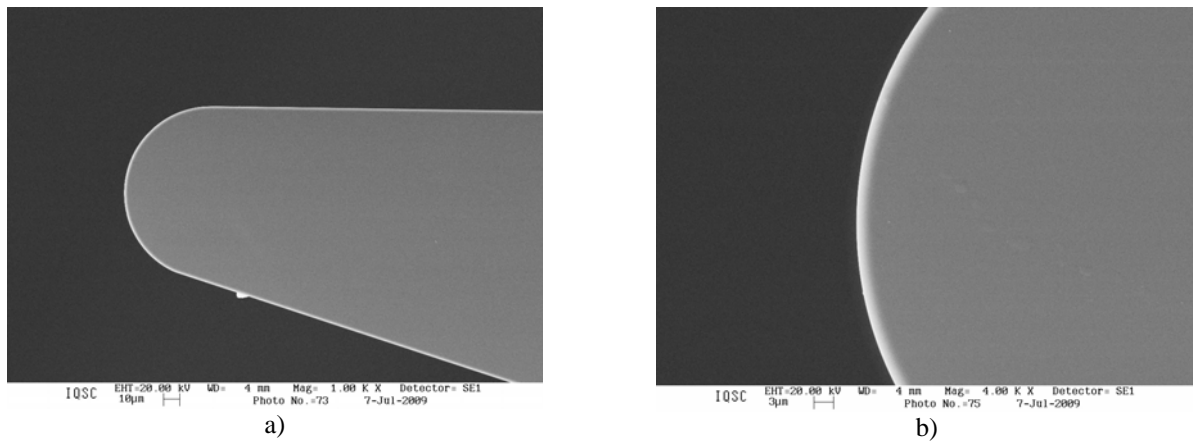


Figure 1. Scanning electron microscopy showing a new diamond tool; a) tool point geometry and; b) cutting edge detail.

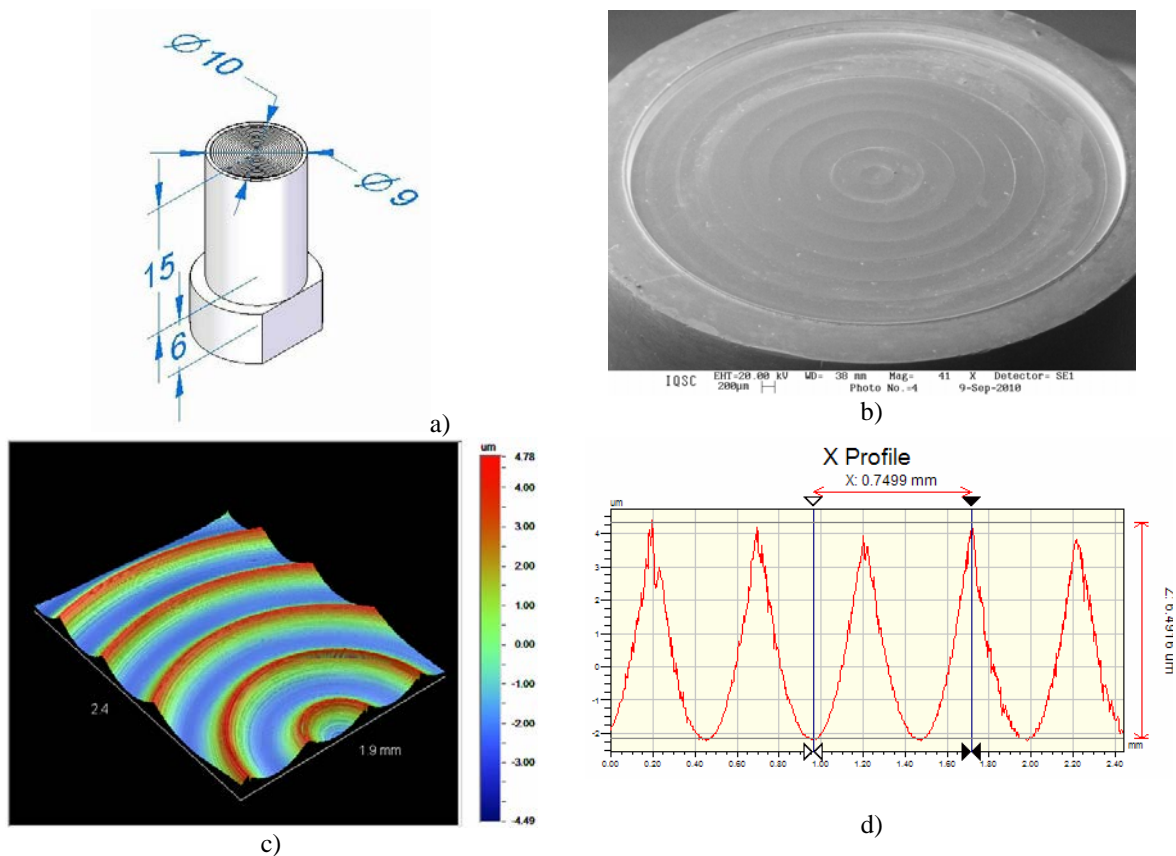


Figure 2. a) Schematic drawing of the copper insert; b) Scanning electron microscopy of the cavity made in the copper inserts with the wavefront structure (Patent PI0201535 8); c) 3D view of the surface topography after diamond turning, and (d) cross-sectional view of the surface roughness profile in the X direction.

3. Experimental Results

Diamond tool wear

Figure 3 (a) shows a typical continuous ribbon-like chip removed during the machining test. Figure 3(b) is the surface microtopography and morphology of the lamella structure. It can be seen that the lamella thickness varies from grain to grain. This is a result of the random crystallographic orientation of the crystal grains.

R.G. Jasinevicius, R.M. Granado and G.A. Cirino
Diamond tool wear analysis

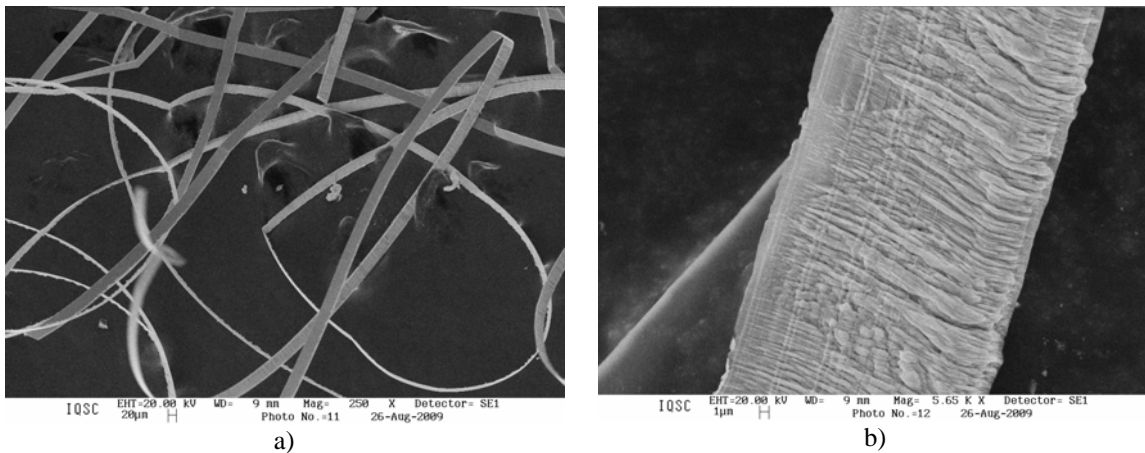


Figure 3. SEM photomicrograph of chips; a) general view and; b) enlarged view of the free surface of the chip showing the lamellar structure.

Figure 4 is a scanning electron microscopy of the tool wear after 2.5 km with different feedrates (cavity and microstructure). As shown in Fig. 4 (a) there is a clear wear of the nose radius but no signs of cratering were detected on the rake face. The main tool wear pattern is flank wear very similar to the flank wear pattern shown in ANSI/ASME B94.55M-1985 standard (1985). The value of the maximum flank wear (VB shown in Fig. 4(b)) measured in the clearance surface is 22 micrometers. It is worth mentioning that hitherto there is no determined value of VB for flank wear for this special tool geometry. In Figure 4(b), on the left portion of the flank face a groove can be noticed.

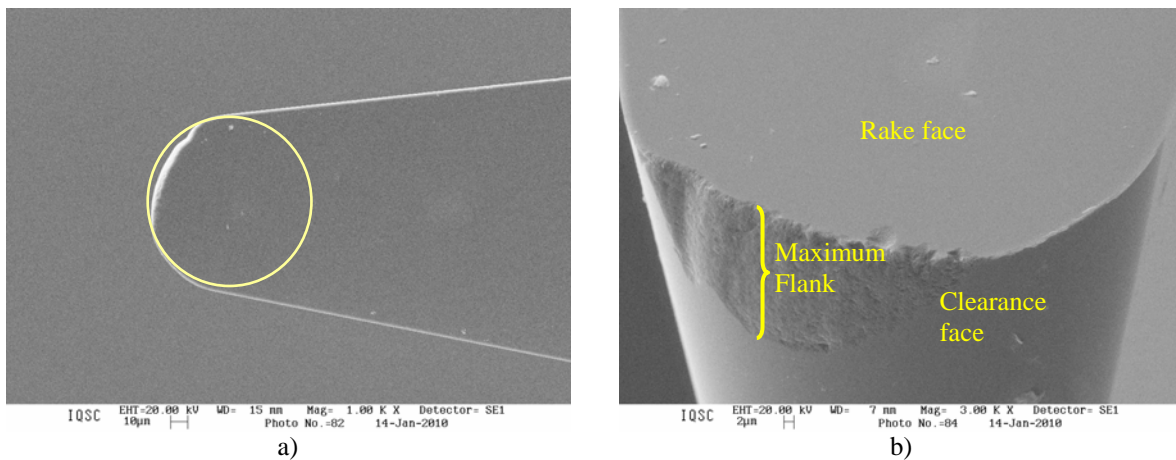


Figure 4. SEM photograph of the cutting tool after machining tests; a) tool nose radius showing a retraction due to wear and; b) tool clearance face showing flank wear and groove on the left portion.

The main concern in diamond-tool pre-selection is the quality of the surface produced as reported by Hurt and Showman (1986). Experience has shown that small nicks formed on the tool edge result in the primary roughness on the finished optical surface. These nicks need only be a few hundred angstroms in dimension and are therefore impossible to be seen under optical microscope. In theory, nicks could be seen under high resolution scanning electron microscope. However, in a manufacturing environment, it is not economical to make a large investment to characterize the tool edge. The authors mentioned previously have proposed a simple method to inspect the cutting edge quality, named: the “fingerprint test”. This test involves machining at high surface speed and very fast feed rates. Each machining groove is the replication of the diamond tool edge at the nose. Even the smallest of the nicks in the edge produces lines on the surface that are easily resolved by an optical profiler. Since the tool used has a very small nose radius the feed rate was not so large, i.e., 12.5 micrometers per revolution. Figure 5 shows an array of SEM image along with optical profiler result of the fingerprint test result. Figure 5 (a) is a SEM photomicrograph of the worn tool with indication of the main nicks (pointed as numbers 1, 2 and 3). Figure 5 (b) is an optical profiler’s trace of the fingerprint grooves showing the isolated nicks marked in (a) as 1, 2 and 3 reproduced on them; and Fig.5 (c) the cross section of the surface showing the fingerprint of the nicks generated within the cutting grooves.

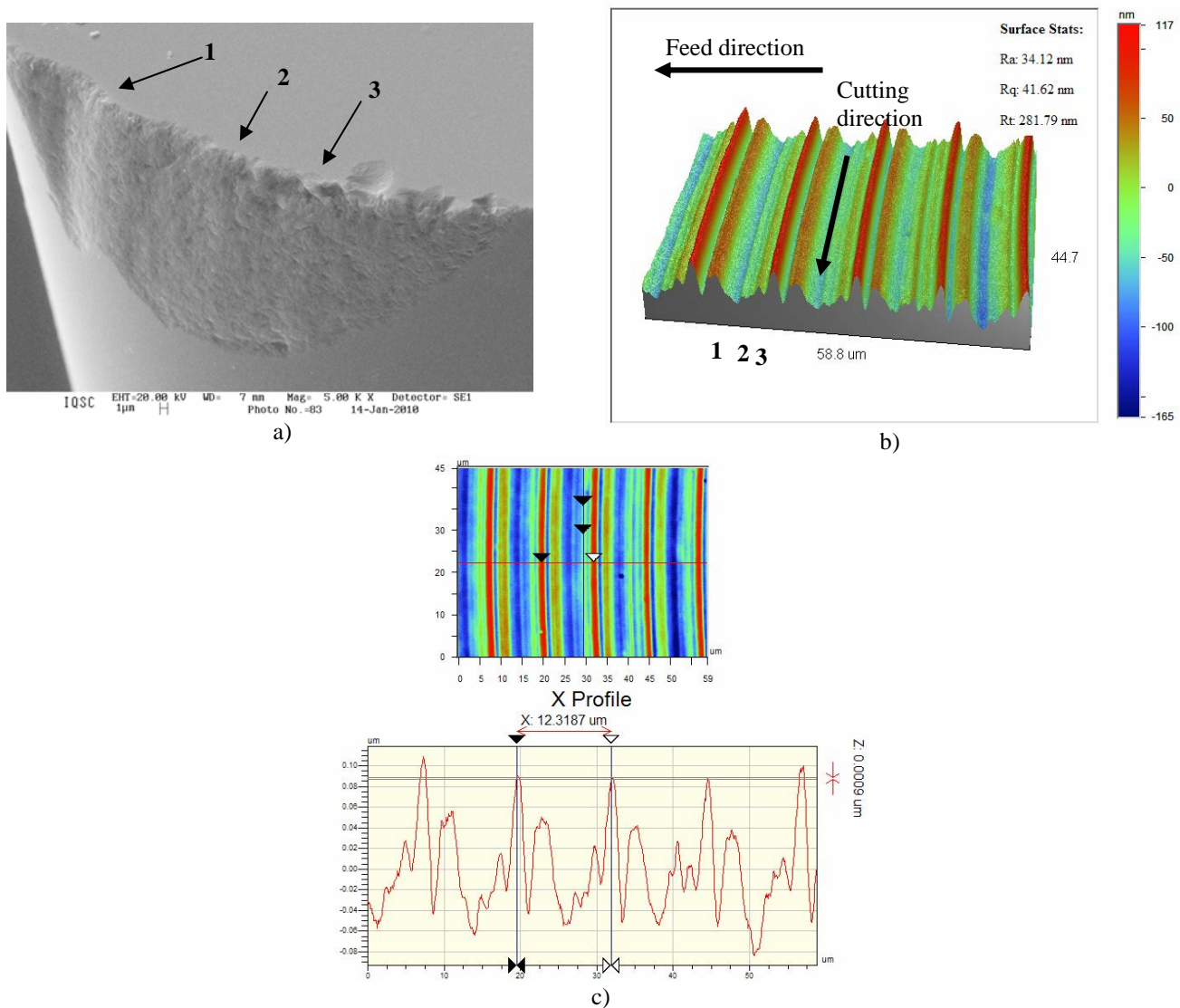


Figure 5. Fingerprint test result of the worn diamond cutting edge; a) scanning electron micrograph of the diamond cutting edge showing the major nicks and flank wear (note the eroded groove on the left portion of the edge) and; b) an optical profiler 3D image of the fingerprint grooves showing the isolated nicks marked in (a) as 1, 2 and 3 reproduced on them; c) cross section profile of the surface.

4. Discussion

In ultraprecision machining of mirrors, the typical cutting conditions, i.e., feedrate and depth of cut, when large nose radius (0.5-1.5 mm) tool is used, range from 5-15 $\mu\text{m}/\text{rev}$ and 1-10 μm , respectively. This order of magnitude implies that material removal and surface generation be governed by the micro interaction between the diamond cutting edge and the workpiece material as previously discussed by Jasinevicius et al (1999). In the machining of polycrystalline materials, the cross section of the chip will be within the domain of a single crystal, as shown in Figure 6. Figure 6 (a) gives the schematic diagram illustrating the interaction of cutting edge and a single grain since the dimensions of the machining are typically smaller than the average size of the crystal grains. It is possible to observe that a single grain shows several grooves (Fig. 6 (b)). Figure 6 c) shows the difference in height from one grain to the other due to the difference in elastic properties in each grain.

The cutting process produced two wear zones (as shown in Fig. 4), namely: tool flank wear and grooving (at the outer edge of the cut). The groove did not seem to affect the surface finish (small tool nose radius and very small feed rate) and was not particularly harmful, except in the case of the fingerprint test shown in Figure 5. The small groove observed on the flank face may be attributed to the interaction between the tool and the outmost work hardened layer of material. This groove may be attributed to a combination of abrasion and attrition which are strongly influenced by the interactions with the atmosphere as well discussed by Trent and Wright (2000). Besides the presence of a work-hardened layer on the previously cut surface, stress concentration due to the stress gradient at the free surface and the

presence of an (abrasive or reactive) an oxide layer on the previously cut surface can also affect the cutting edge integrity (Shaw et al, 1966).

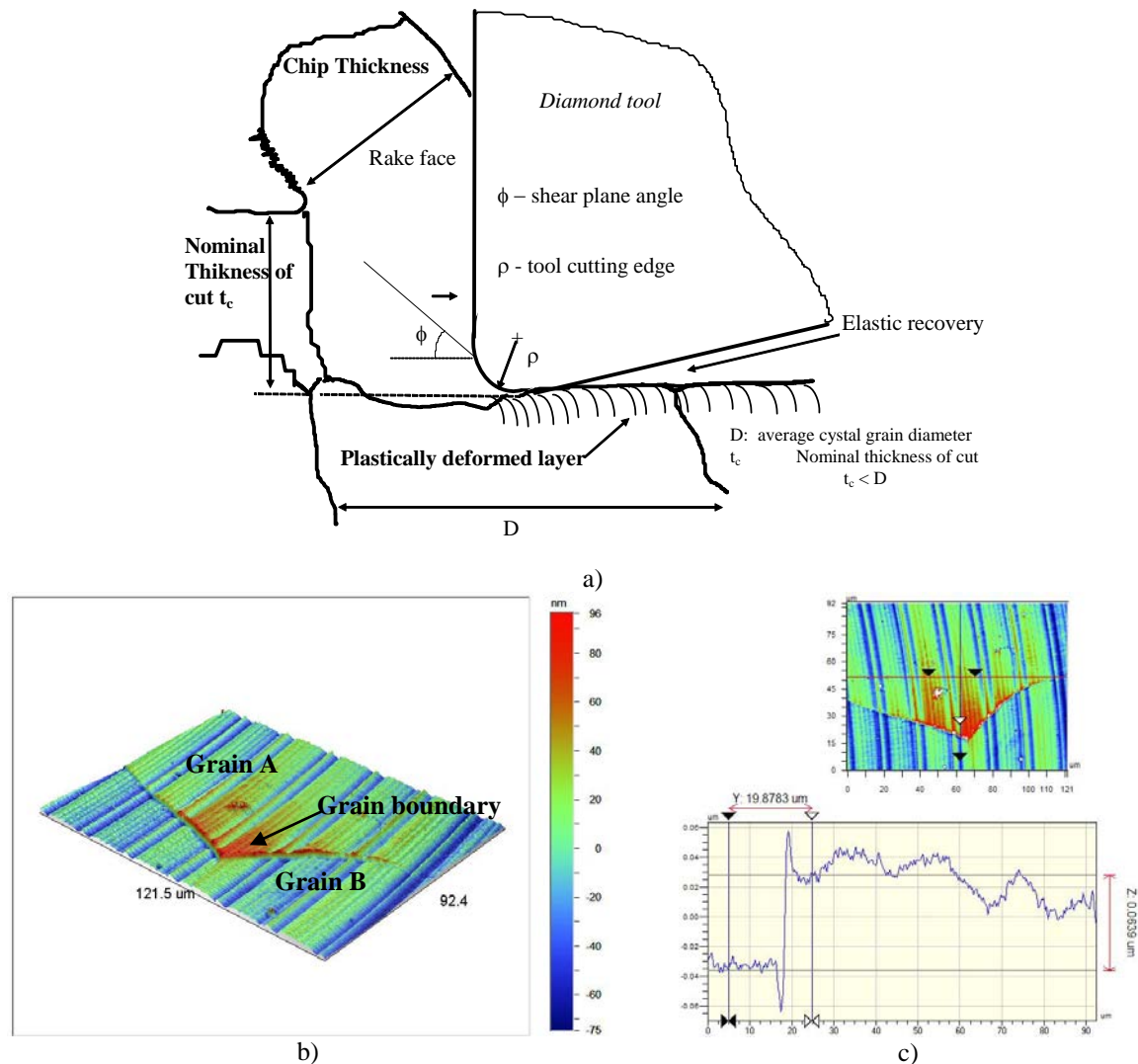


Figure 6. The machining conditions are smaller than the average grain size. (a) schematic diagram showing the cut in only one crystal grain; (b) 3D image obtained by means of an optical Profiler showing that a single grain shows several grooves left by the tool; (c) cross section view of the surface where is showed the step generated from one grain to the next due to the difference in elastic modulus. Material: Commercially pure Copper.

Figure 7 shows the microhardness of the machined samples. The microhardness values of the machined sample are always larger than those of the *as-received* material. When the penetration is low ($0.88 \mu\text{m}$ at 5 grams and maximum of $7.47 \mu\text{m}$ at 200 grams) the micro indentation occurs within the work hardened layer generated by the tool/workpiece material interaction during cutting. This damaged layer is very thin, i.e., in accordance with reported works on work hardening after diamond turning of non ferrous metals (e.g. Al, Cu, etc.), where the depth of the work hardened layer was in the range of 1 to $17 \mu\text{m}$ as reported by Evans et al (1986) and Horio et al (1992). As the indentation load increases, the work hardened layer effect upon micro hardness is attenuated. For higher loads, e.g., 200g, the surface micro hardness of the machined sample and the as-received samples are similar.

Figure 8 gives the schematic diagram illustrating the machining geometry with a round nose tool. In subsequent passes the cutting edge will be cutting a layer of material with different hardness (Fig.8 (a)), since a plastically deformed layer will be formed. Drescher and Dow (1990) have proposed a model showing the interaction between the tool edge and chip geometry with a representation of material hardness profile (Figure 8 (b)). In Fig. 8 (b): D is the overall depth of cut which is generally large relative to ρ , the extent of plastic work. The hardness, H , is an exponential function of d (depth below the line S) which is the surface created by the preceding tool pass, f is the feed rate (in, for example, $\mu\text{m rev}^{-1}$). The wear pattern of the flank face can be determined by this hardness distribution. According to Zorev (1966), the normal and frictional forces on the tool flank acting at the tool-workpiece interface will determine the

contact processes on the tool flank. Due to the complexity of the contact on this interface (particularly when the nose radius is very small as in the case studied in this work), the ratio of the normal and contact forces does not follow those obtained in standard machining tests where severe friction and plastic deformation are present. It has to be mentioned that the specific cutting energy in our tests is much larger than in conventional diamond turning process because of the small nose radius and cutting length. According to several reported works, the total specific energy involved in diamond turning of copper with conventional nose radius tools at depth of cut of 10 μm is 2 GPa (Moriwaki et al, 1993; Ueda et al, 1998).

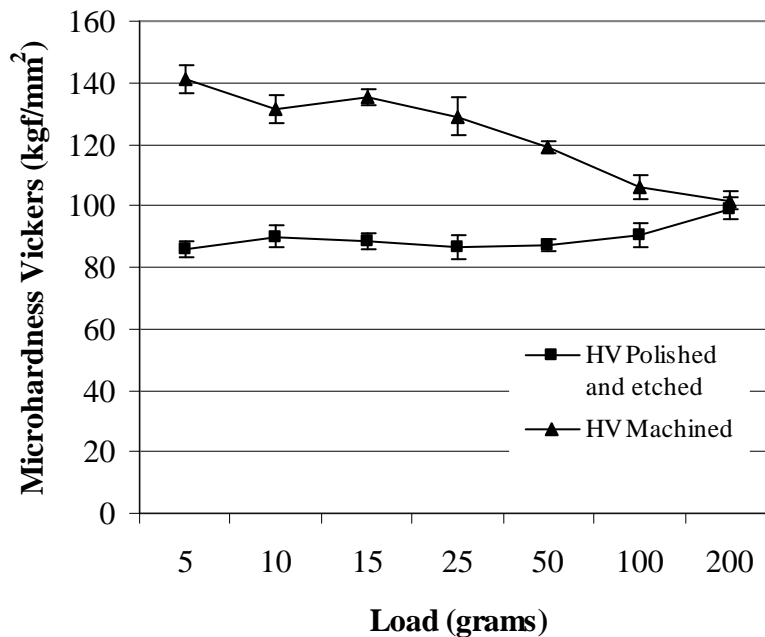


Figure 7. Microhardness Vickers of commercially pure copper used in the cutting tests measured before and after machining.

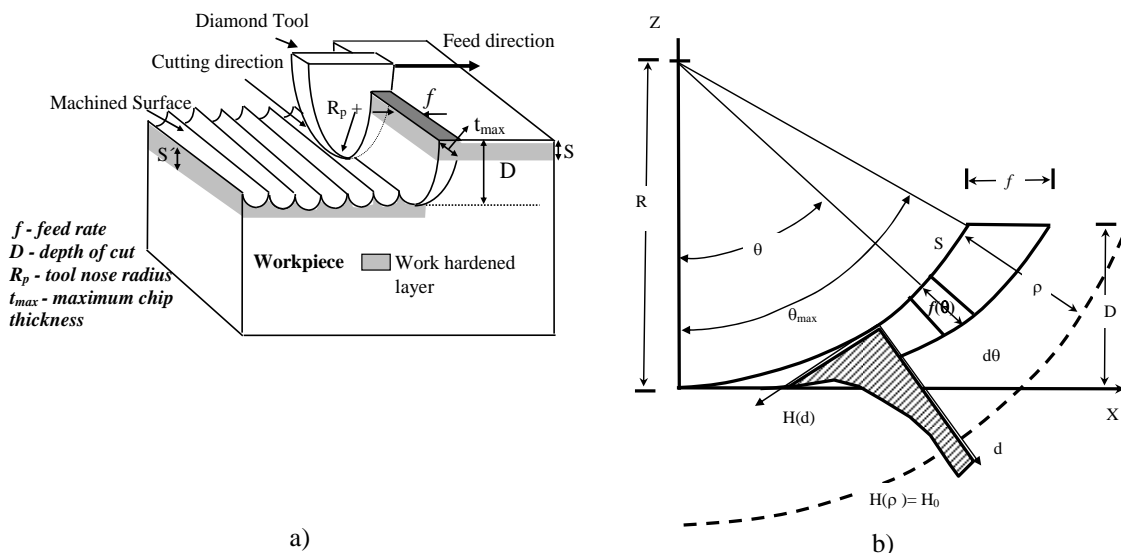


Figure 8. The machining conditions are smaller than the average grain size. (a) Schematic diagram illustrating machining geometry with round nose tool and the formation of a work hardened layer induced by machining; (b) schematic diagram showing chip geometry with representation of material hardness profile (after Drescher and Dow, 1990).

Cutting tool wear results from a combination of mechanisms involved during machining. In our case two facts must be considered: commercially pure copper includes oxygen as an impurity and the estimated temperature during diamond

turning of copper is much lower than this value, and it was estimated in the range of 500 to 550 K (Lucca et al, 1991; Lucca and Seo, 1993). When carbon atoms on the diamond surface react with oxygen in a deoxidization process, a copper oxygen- carbon complex may be formed on the tool-work interface as described by Paul et al. [17]. According to Shimada and collaborators (2000), carbon atoms in the diamond surface can be removed under the contact with copper, due to oxidization accompanied with deoxidization of copper oxide. This can occur even at considerably low atmospheric temperature at which diamond is not oxidized by itself. Copper in this case could be considered to act as a catalyst. The volumetric wear of diamond increases as the increase of atmospheric oxygen partial pressure around the contact region between diamond and copper. This reaction might be one of the mechanisms responsible for the flank wear observed. Consequently, carbon atoms in the tool surface could be removed due to oxidization, accompanied with deoxidization of copper oxide, by diamond under the cited cutting temperature suggested by the results of thermodynamics analysis shown by the previously cited paper. Ultimately, it is worth mentioning that in general it is suggested that between 80% to 85% to be the amount of heat removed by diamond. However, according to Carr and Feger, (1993) there is a decrease in the absolute value of thermal conduction with the increase of temperature. In the case of the material being cut here the change may be considered minimal, albeit fairly large for diamond. At 200°C above ambient the thermal conductivity of diamond is reduced to roughly half of its previous amount over its room temperature value. Consequently, copper will remove a larger fraction of the heat which may influence the thermal expansion and increase in the friction of the formed machined surface and the tool clearance face.

All these aspects treated here might be considered responsible for the premature and deleterious wear observed on the tool flank face.

5. Conclusions

Tool wear in ultra-precision diamond cutting of commercially pure copper inserts with a special geometry tool (small round-nose) for the machining of a wave front sensor was studied based upon tool/material interaction in the micro-cutting process. The cutting tool wear pattern was investigated based upon the observation of the worn region using scanning electron microscope. The zero degree rake angle single point diamond tool presented small groove on the flank face. No wear was detected on rake face of the diamond tool. Fingerprint test was carried out in order to replicate the profile of the wear pattern. Three dimensional view of the wear pattern was showed by means of an optical profiler image. The micro hardness of copper sample increased after machining. It was considered that this work hardening might have contributed for the groove wear pattern observed at the outer edge of the tool. The wear pattern observed on the flank surface was attributed to a combination of wear mechanisms, to know: abrasion and attrition. The flank wear mechanism was attributed to the presence of atmospheric oxygen around the contact region between diamond and copper. The carbon atoms on the tool surface could be removed due to oxidization, accompanied with deoxidization of copper oxide according to reported works in literature (Shimada et al 2000).

Acknowledgements.

This work was supported by the Brazilian research financing agencies FAPESP – Fundação de Amparo a Pesquisa do Estado de São Paulo (Process No. 2008/53641-5) and CNPq – Conselho Nacional de Desenvolvimento Científico e Tecnológico (Process No. 472334/2008 5).

References

- American National Standard ‘‘Tool Life Testing With Single- Point Turning Tools’’ ANSI/ASME B94.55M-1985’’, ASME, New York, 1985.
- Bex, P.A., (1975) Diamond turning tool. *Industrial Diamond Review*, pp.11-18.
- Carr, J.W., Feger, C., *Ultraprecision machining of polymers*, *Prec. Engg.*, Vol.15(4):221-227, 1993.
- Davies, M. A., Evans, C. J., Patterson, S. R., Vohra, R., Bergner, B. C. (2003) Application of precision diamond machining to the manufacture of micro-photonics components. *Proc. of SPIE Lithographic and Micromachining Techniques for Optical Component Fabrication II*, edited by E.-B. Kley, H. P. Herzig (SPIE, Bellingham, WA, 2003) · 0277-786X/03Vol. 5183, pp.94-108.
- Drescher, J.D., Dow, T.A. (1990) Tool Force Model Development for Diamond Turning”, *Precision Engineering*, Vol. 12 (1):29-35.
- Evans, C.; Polvani, R.; Postek, M., Rhorer, R. (1987). Some observations on tool sharpness and subsurface damage in single point diamond turning”. *SPIE – In Process Optical Metrology for Precision Machining*, v. 802, p. 52-66.
- Falldorf, C., Dankwart, C., Gläbe, R., Lünemann, B., Kopylow, C.v., Bergmann, R.B. (2008) Holographic projection based on diamond-turned diffractive optical elements. *Applied Optics*, Vol. 48, No. 30 / 20: 5782-5785.
- Horio, K.; Kasai, T.; Ogata, Y.; Kobayashi, A. (1992) A study on damaged layer remaining in diamond mirror cut surface. *Annals of the CIRP*, v. 41, n. 1, p. 137-140.
- Hurt, H.H., Decker, D.L., (1984) Tribological considerations of the diamond single point tool. *SPIE Production Aspects of Single point machined optics*, Vol. 508, pp.126-131.

- Hurt, H. H., Showman, G.A., (1986) Wear test of a preselected diamond tool. SPIE Ultraprecision machining and Automated Fabrication of Optics, Vol. 676, pp.116-124.
- Jasinevicius R.G. Porto A. J. V., E Duduch J.G. E Purquerio, B.M. (1999) Critical Aspects on the Behaviour of Material from the Mechanical Tool-Workpiece Interaction in Single Point Diamond Turning. Journal of the Brazilian Society of Mechanical Science. Vol.21 (3): 509-518.
- Leung, H. M., Zhou, G., Yu, H., Chau, F.S., Kumar, A.S. (2009) Liquid tunable double-focus lens fabricated with diamond cutting and soft lithography. Applied Optics, Vol. 48, No. 30 / 20: 5733-5740.
- Lucca, D.A., Rhorer, R.L., Komanduri, R. (1991) Energy dissipation in the ultra-precision machining of copper". Annals of the CIRP, Vol. 40 (1): 69-72,
- Lucca, D.A., Seo, Y.W. (1993) Effect of Tool Edge Geometry on Energy Dissipation in Ultraprecision Machining. Annals of the CIRP, Vol. 42 (1): 83-86.
- Moriwaki, T., Sugimura, N., Luan, S. (1993) Combined Stress, Material Flow and Heat Analysis of Orthogonal Micromachining. Annals of the CIRP, 4211: 75-78.
- Paul, E., Evans, C.J., Mangamelli, A., McGlaulin, M.L., Polvani, R.S., (1996) Chemical Aspects of Tool Wear in Single Point Diamond Turning, Precision Engineering, Vol.18(1): 4-19.
- PI0201535 8 Dispositivo sensor de frentes de onda com simetria cilíndrica para medir aberrações ópticas.
- Qin, Y., Brockett, A. Ma, Y., Razali, A., Zhao J., Harrison, C., Pan, W., Dai, X. Loziak, D. (2010) Micro-manufacturing: research, technology outcomes and development issues. Int. J. Adv. Manuf. Technol., Vol.47:821–837
- Rakuff, S., Beaudet, P. (2008) Thermal and Structural Deformations During Diamond Turning of Rotationally Symmetric Structured Surfaces. Journal of Manufacturing Science and Engineering, Vol. 130: 041004-1 - 041004-9.
- Sahli, M., Millot, C., Roques-Carmes, C., Kahn-Malek, C., Bariere, T., Gelin, J.C., (2009). Quality assessment of polymer replication by hot embossing and microinjection molding using scanning mechanical microscopy, J. Mater. Process. Technol., 209: 5851-5861.
- Shaw, M.C., Thurman, A.L., Ahlgren, H.J. (1966) A plasticity problem involving plane strain and plane stress simultaneously: groove formation in the machining of high temperature alloys. Trans. of the ASME – Journal of Engg. For Ind., vol. 88(2) pp.142-146.
- Shimada, S., Inamura, T., Higuchi, M., Tanaka, H, Ikawa, N. (2000) Suppression of Tool Wear in Diamond Turning of Copper under Reduced Oxygen Atmosphere. Annals of the CIRP Vol. 49 (1): 21-24.
- Tanaka, H., Shimada, S., Higuchi, M., Yamaguchi, T. Kaneeda, T., Obata, K. (2005) Mechanism of Cutting Edge Chipping and Its Suppression in Diamond Turning of Copper. CIRP Annals - Manufacturing Technology Volume 54(1): 51-54
- Tofteberg, T., Amedro, H., Andreassen, E. (2008) Injection Molding of a Diffractive Optical Element. Polymer Engineering and Science., pp. 2134-2142.
- Trent, E.M., Wright, P.K., (2000) Metal Cutting. 4th edition Butterworth & Heinemann Press, 446p.
- Ueda, T., Sato, M., Nakayama, K. (1998) The Temperature of a Single Crystal Diamond Tool in Turning, Annals of the CIRP, 47/1: 41-44.
- Wong, C.J. (1981) Fracture and Wear of Diamond Cutting Tools. Trans. of the ASME, J. Engineering Materials and Technology, Vol.103, pp.341-345, Oct. 1981.
- Yin, Z. Q., To, S., Lee, W.B., (2009) Wear Characteristics of diamond tool in ultraprecision raster milling. Int. J. Adv. Manuf. Technol., vol. 44:638-647.
- Yoshikawa, T., Kuoi, M., Maeda, y., Ohta, T., Taya, M., (2009) Ultraprecision machining of dies for microlens arrays using a diamond cutting tool. *Key Engineering Materials, Vols. 407-408 pp 359-362.*
- Zhang, H., Zhou, M. (2010) Tool Wear in Diamond Cutting Sinusoidal Microstructured Surfaces. *Key Engineering Materials, Vols. 431-432 pp 94-97.*
- Zhou, M., Ngoi, B.K.A., Wang X.J. (2003) Tool wear in ultra-precision diamond cutting of non-ferrous metals with a round-nose tool. Tribology Letters, Vol. 15 (3):211-216.
- Zorev, N.N. (M.C. Shaw, Trans.) (1966) Metal Cutting Mechanics, Pergamon Press, Oxford.

RESPONSIBILITY NOTICE

The author(s) is (are) the only responsible for the printed material included in this paper.